EUROPEAN COMMISSION
5th EURATOM FRAMEWORK PROGRAMME 1998-2002
KEY ACTION : NUCLEAR FISSION

HTR-N

HTR-N & N1
High-Temperature Reactor Physics and Fuel Cycle Studies
(EC-funded Projects: FIKI-CT-2000-00020 & FIKI-CT-2001-00169)

Work Package: 1	HTR-N project document No.: HTR-N1-03/06-S-1.1.3-1_1				Q.A. level: 1
Task: <1.1.1>	Document type: Support document				Document status: final
Issued by: CEA	original document No.:	Annex pg. 0	Rev. 0	Q.A. level n/a	Dissemination level: CO

Document Title

CEA Calculational Results for the HTTR Benchmark Problems

Author(s)

F. Damian, X. Raepsaet

Organisation, Country

CEA - France

Notes

Electronic filing: ***SINTER***

Electronic file format: ***PDF file***

Rev.	Date	Short Description	Prepared by	Partners' Review	Control WP Manager	Approval Project Manager
					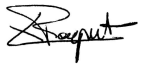	
0	5-06-2003	first issue	CEA		CEA X. Raepsaet	FZJ von Lensa

Chronology and history of revisions

Rev.	Date	Description
0	5-06-2003	First version

GENERAL ANALYSIS METHOD AND MODEL DESCRIPTION

CODES AND CALCULATION SCHEME

In the following HTTR calculations, the French reactor physics code system SAPHYR has been used. SAPHYR gathers several codes developed at CEA like APOLLO2 [3] (transport) based on a database produced with THEMIS/NJOY, CRONOS2 [4] (diffusion-transport), FLICA4 (3D-thermal hydraulics), ..., which are interconnected. This code system, initially dedicated to PWR calculations and research & development purposes, seems to be well adapted for the assessment of the HTGR performances and characteristics. Finally, the Monte-Carlo code TRIPOLI4 [5] has also been used throughout the study.

All the HTTR problems proposed in reference [1] have been treated considering two calculation methods: one based on a Transport – Diffusion calculation scheme and a second one based on a Transport – Monte-Carlo calculation scheme. Figure 1 illustrates the general procedure. The standard 172-groups or point-wise cross sections library issued mainly from JEF-2.2 are used for the calculations.

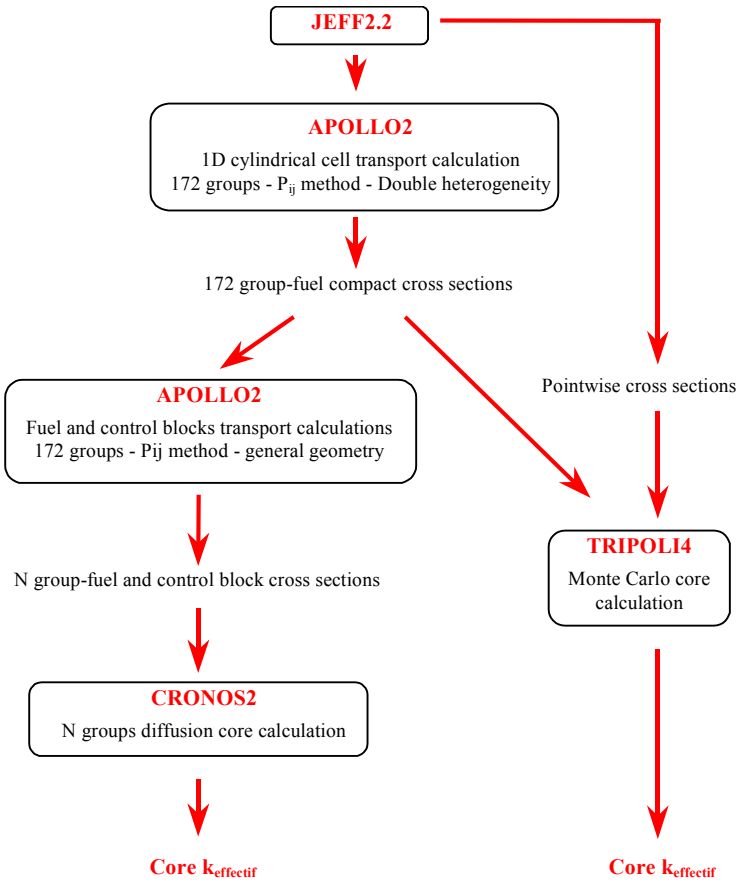

FIG. 1. Description of both calculation schemes

It is noteworthy that as far as the Transport-Diffusion calculations are concerned, two different approaches have been used in terms of core modelling. The first one, a rough model with strong hypotheses (homogenised fuel block, no streaming effect, …) led to preliminary predictions of the HTTR-FC, EX and CR problems (**first results**). Then, enhancements to improve the modelisation have been identified, assessed and finally implemented in course of revised calculations using new

benchmark data proposed in [7]. This has been done for all the HTTR benchmarks (FC, EX, CR, SC and TC) and constitutes the second prediction (**final results**).

CYLINDRICAL CALCULATION OF THE FUEL COMPACT

Knowing that the stochastic geometries calculations (coated fuel particles - CFP - randomly distributed in the fuel compact) is not available in the Monte-Carlo code TRIPOLI4, a 1D-cell calculation has been performed as a first step. It takes into account a precise spherical description of the particles with all their coatings which themselves fill the annular part of the cylindrical geometry of the fuel compact (Fig. 2) with a packing density around 30 %. The self-shielding of the uranium is calculated during this calculation stage. A collision probability method is used to solve the transport equation with 172 energy groups. The critical buckling search allows taking into account the neutron leakage by the addition of an homogeneous leakage term in the form of $DB^2\Phi$. The extra region of the cylindrical cell is representative of the other fuel cells disposed around with the triangular pitch of the fuel rods in the assembly.

FIG. 2. Cylindrical Fuel Cell Model

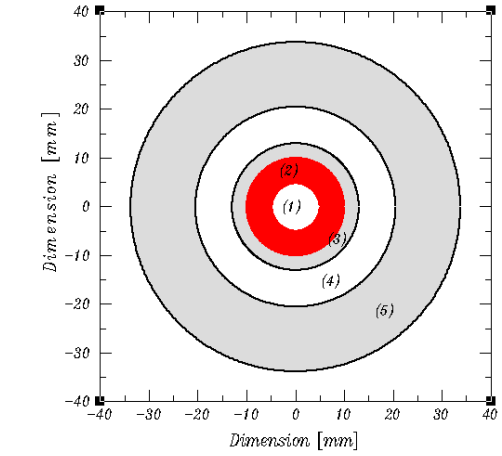

(1) Helium
(2) Fuel
(3) Graphite
(4) Helium
(5) Extra-region

This first stage provides **fuel compact-homogenized 172-group cross sections** for Monte-Carlo core calculations (TRIPOLI4). Therefore, in the core calculations performed by TRIPOLI4, pointwise cross sections are used everywhere in the core except in the fuel rod region where the multigroup cross sections have been generated with APOLLO2.

Although that the CFP might be directly considered in the 2D fuel element calculations, as for TRIPOLI4 the same **fuel compact averaged 172-group cross sections** have been used in the 2D transport model described hereafter. This avoids calculating the self-shielding in the 2D configuration and results in a large saving of CPU time without making severe assumption.

FUEL BLOCK 2D-CALCULATIONS

This stage must lead to an averaged flux weighted library of the different fuel blocks existing in the core. This library of n-group-constants is directly read during the core diffusion calculations. The

energy structures (n = 2 to 20) are given in annexe. A 172 group-collision probability method is used in the 2D-fuel block geometry (Fig. 3). The fuel handling hole zone is modelled by a lower graphite density. As far as the burnable poisons (BP) are concerned, the B_4C and graphite pellets are **axially homogenised** with the graphite matrix in order to reduce the number of calculations from 32 to 16 and to simplify the core calculations. The impact of this axial homogenisation is important and has been evaluated hereafter.

FIG. 3. 2D-fuel block geometry

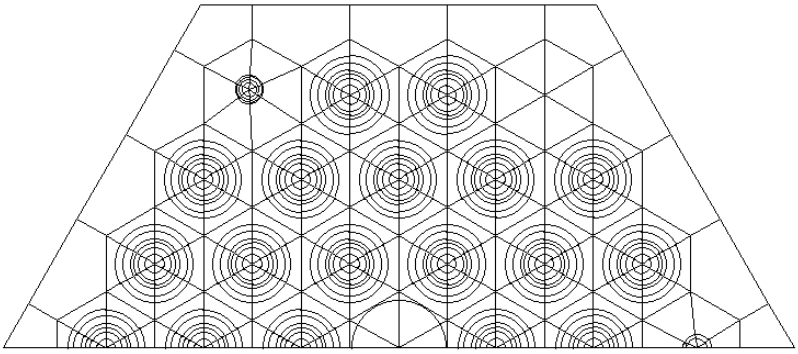

These 2D calculations were performed in infinite medium with a critical buckling search. A B1 homogeneous neutron leakage model has been retained as a first step. This led to **isotropic diffusion coefficients** and did not allow taking into account the streaming effect. The P_{ij} model gives a flux evaluation in each region depicted in Fig. 3. An example of the power distribution in a fuel block is given in Fig. 4 (the map is normalised to 100).

FIG. 4. Power Distribution in the f343320 fuel block

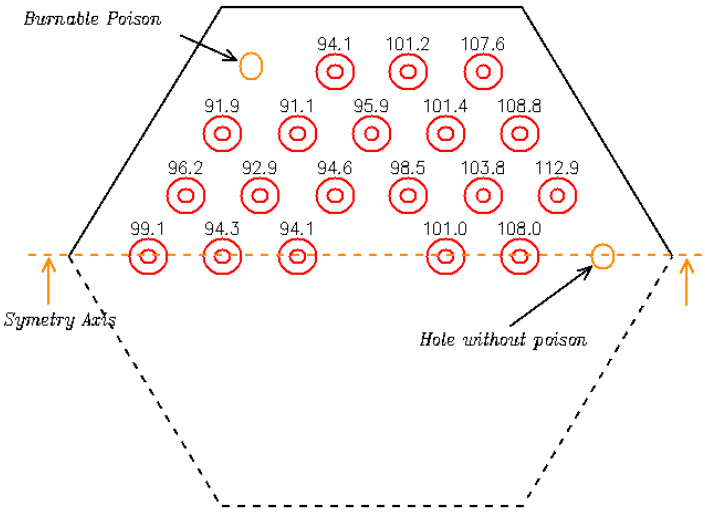

The 2D-results of the fuel blocks in fundamental mode are gathered in the Table 1 below and an example of the average neutron flux obtained for the lower and the higher enriched fuel blocks are given in Fig. 5.

TABLE 1 2D-TRANSPORT CALCULATIONS ON THE FUEL BLOCKS

Fuel Block	Enrichment [% masse]	Multiplication factor	Migration Area [cm^2]
f343320	3,4	1,10650	491,05
f393320	3,9	1,14991	487,14
f433120	4,3	1,18391	486,43
f483120	4,8	1,21366	481,82
f433325	4,3	1,15656	476,90
f523325	5,2	1,20380	470,53
f593125	5,9	1,24481	469,50
f633125	6,3	1,25798	468,43
f633325	6,3	1,24962	465,50
f723125	7,2	1,28937	463,70
f793125	7,9	1,30862	457,99
f673320	4,6	1,28423	467,60
f793320	7,9	1,31733	459,52
f943120	9,4	1,36335	458,81
f993120	9,9	1,37213	455,45

FIG. 5. Neutron Spectrum in the fuel block

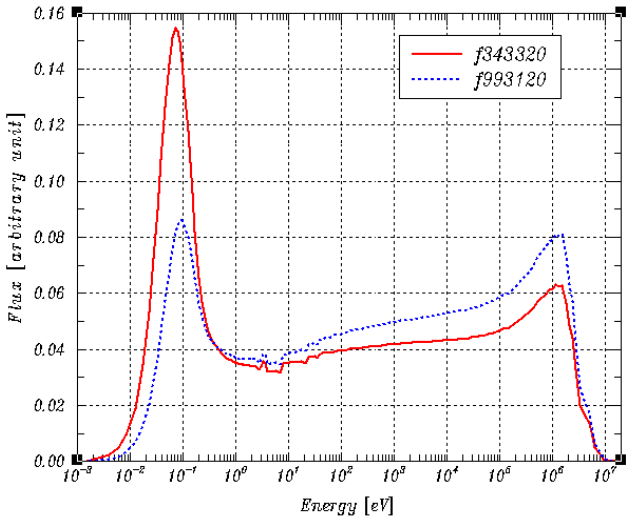

CONTROL BLOCKS 2D-CALCULATIONS

From the previous calculations, the average fluxes of the fuel blocks were used as a 172 group-neutron source placed at the periphery of the control blocks to generate the averaged weighted library needed for core diffusion calculation. A similar collision probability method has been used in the 2D-geometry shown in Fig. 6 for the control blocks with and without the control rods inserted.

As for the fuel blocks, the n-group-constants have been created by spatial homogenisation on the overall control block geometry. Indeed, among the finite element meshes available in the CRONOS2 diffusion code, it was first impossible to take into account the position and the orientation of the fuel and control blocks by an heterogeneous geometric description of these elements. Moreover, no transport-diffusion equivalence factors have been considered for the control blocks when the control rods are inserted. The averaged neutron fluxes obtained in the control blocks are given in Fig. 7.

FIG. 6. 2D-Control Rod Blocks Geometry

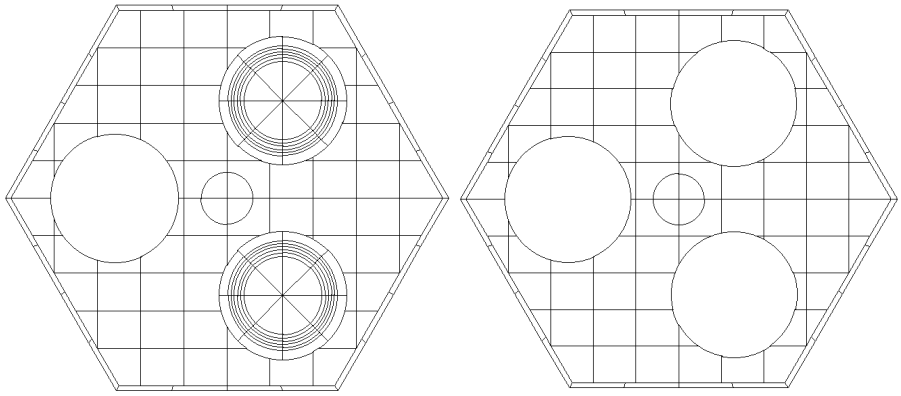

FIG. 7. Neutron Spectrum in the Control Rod Blocks

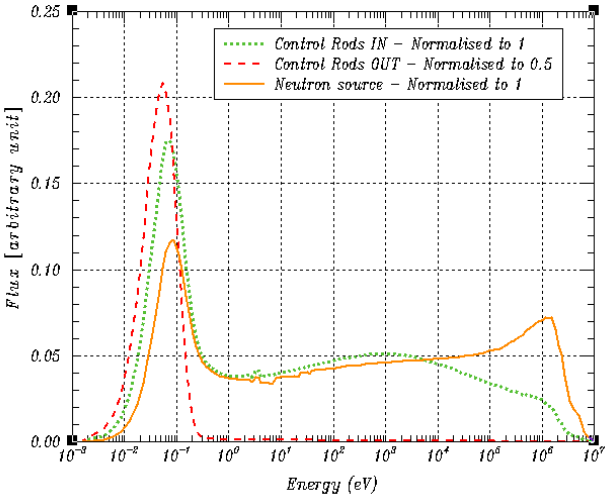

REFLECTOR CROSS SECTION GENERATION

In the diffusion calculations, the n-group-cross sections of the replaceable reflector have been evaluated with similar methods to those described in the previous section where a neutron source is placed at the periphery of the blocks. As far as the permanent reflector region is concerned, the cross sections come from a 1D-cylindrical core transport calculation (in its fully loaded configuration) performed with the S_n method.

CORE DIFFUSION CALCULATIONS

An hexagonal 3D-geometry has been used for the core description. Each fuel and control block is represented by a **hexagon with a homogeneous composition**. On this hexagonal mesh, the *finite element method* provides several polynomial approximations. In this case, a second order exact integration (standard parabolic Lagrange) has been adopted horizontally and leads to 19 flux values per mesh (equivalent to a 24 homogeneous meshes in finite difference method).

FIG. 8. Core Axial Description for CRONOS2 code

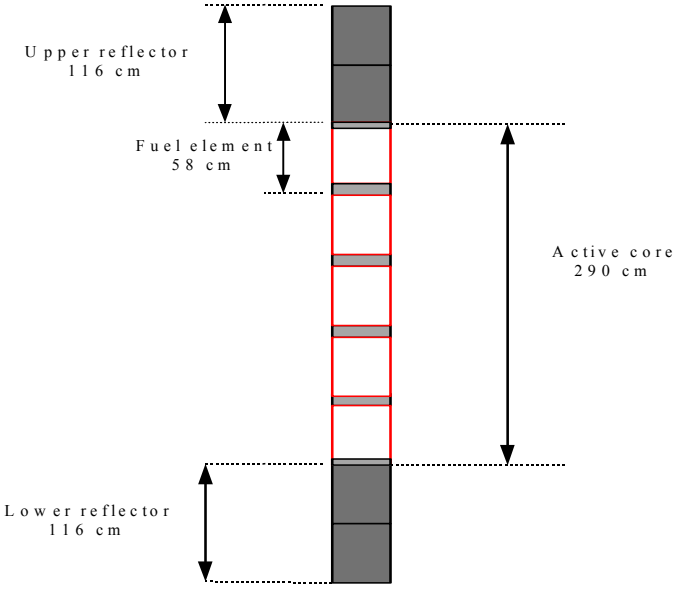

Axially, a linear Lagrange method using Gauss Formula has been applied. Each fuel section (14 fuel compact stack) was divided into 6 meshes and the inter-space between these fuel sections (3.4 cm of graphite) has been described explicitly as shown in Fig. 8.

TRANSPORT-MONTE CARLO CORE CALCULATIONS

In spite of the homogenised fuel compacts, the core model developed here is a very detailed 3D-model of the HTTR with all components modelled explicitly. For these components, point-wise cross sections based on the JEF2.2 evaluation were used. The fuel compact was represented by a set of 172-group-constants coming from the previous transport calculation. It is noteworthy that in this case the burnable poison had the exact axial description in opposition to the homogeneous axial description used in the core diffusion calculations.

FIG. 9. Cross Section of Fully Loaded Core for TRIPOLI4 code

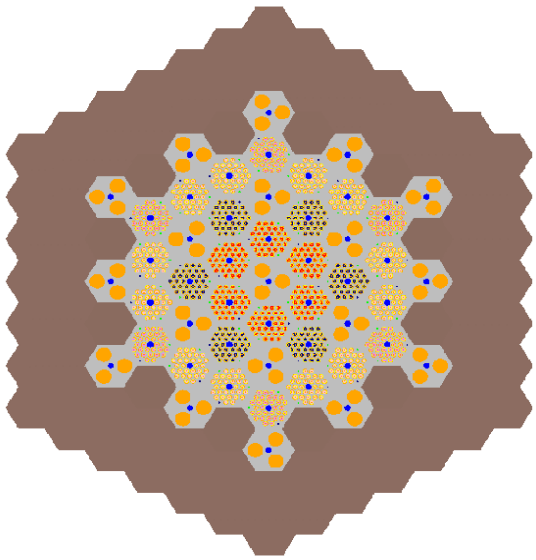

Only the core configurations with 18 and 30 columns have been considered here. Figures 9 and 10 show a cross section view of the fully loaded core and detailed axial and radial cross section views of the control rod and fuel blocks.

FIG. 10. Details of the Geometry used in the TRIPOLI4 code

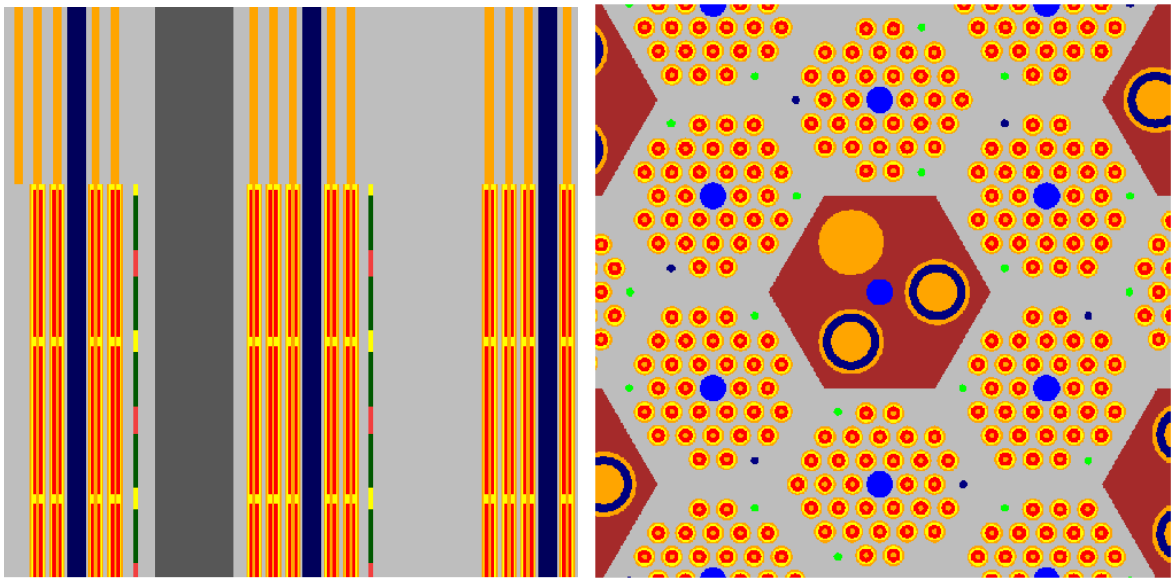

SYNTHESIS OF THE ASSUMPTION OF THE INITIAL DIFFUSION CALCULATION SCHEME

The key factors in modelling the HTTR with the *transport-diffusion* calculation scheme are the following:

- the BP are axially homogenized
- the streaming effect is not taken into account everywhere in the core
- homogenised hexagons are considered without equivalent factor in order to respect the absorption rates of the BP and the control rod (CR) between both transport and diffusion calculation stages
- flux-weighted cross sections are used for the reflector
- CR insertion on the top reflector not taken into account

The following section provides the results taking into account these assumptions. Then, their impacts on the results have been assessed. They have been reconsidered in course of the revised calculations according to the results of these assessments.

FIRST RESULTS

HTTR-FC AND EX

The calculations performed with the two different methods are gathered in Table 2. It is important to note that all the k_{eff}-values of the Table 2 are corrected with a Δk of - 0.004 in order to take into account the presence of the control not fully withdrawn to the top of the reflector and not considered in the core models.

All the preliminary calculations underestimated the number of fuel columns needed to achieve the first criticality (Diffusion calculations: **10 columns**; Monte-Carlo calculations: **17 fuel columns**). As it can be seen in Table 2, the discrepancy between the calculations and the experiment at least ranges from $\Delta k = 0.017$ to 0.058 at 18 fuel columns loading and from $\Delta k = 0.01$ to 0.033 at full core.

It is noteworthy that the observed discrepancies decrease with increasing number of fuel columns in the core. Due to the large experimental uncertainty at 30 fuel columns loading, the differences between the calculations and the experiment are within the error bar, whereas at the thin annular core assembly the discrepancies are significant. Two reasons for the latter circumstance can be proposed. The first would be that the two steps transport-diffusion calculation based on the fundamental mode assumption would be less and less appropriate as one goes toward the annular core configuration. The second would concern the level of the actual boron impurity in the dummy fuel blocks and of the residual air (instead of helium) in the graphite pores. As far as the latter is concerned, the impurities of some dummy fuel blocks have been re-measured by JAERI and revised data [7] have been recommended for the recalculation of the first criticality (HTTR-FC2).

TABLE 2 EXPERIMENTAL, MONTE-CARLO AND FIRST DIFFUSION RESULTS

	CRONOS2 3D - (first model) • *diffusion 8 gr* • *homog. Fuel block* • *no streaming* • *axially homog. BP*	Δk [%Δk/k]	**TRIPOLI4** 3D *Monte-Carlo* *172 gr & pointwise*	Δk [%Δk/k]	**EXPERIMENT**
30 col	**1.1698**	**14.5 %**	**1.14630 ± 0.0009**	**12.8 %**	**1.13630 ± (> 3.6%)**
28	1.1691	14.5 %			
26	1.1596	13.8 %			
24	**1.1399**	**12.3 %**			
22	1.1158	10.4 %			
20	1.0886	8.14 %			
19	1.0745	6.93 %			
18 col	**1.0580**	**5.48 %**	**1.01710 ± 0.0009**	**1.68 %**	**subcritical**
16	1.0383	3.69 %			
14	1.0284	2.76 %			
12	1.0184	1.81 %			
10	1.0044	0.44 %			
9	.9970	- 0.3 %			

In the course of the studies, the following reasons for the above mentioned discrepancies (especially for the simplified Transport – Diffusion calculation scheme) have been identified and quantified:

- A non-adequate treatment of the axial self-shielding in the BP rods,
- An underestimation of the neutron streaming (due to large channels of the CR blocks),
- The neglect of the detailed structure of the HTTR fuel block in the core calculations.

These main physical effects and their impacts on the core reactivity are briefly depicted in Fig. 11 for the case of the annular core configuration. Similar tendencies can be observed for the full core configuration. Nevertheless, different absolute values (into bracket Fig. 11) are obtained for the quantified physical effects due to the harder neutron spectrum in the fully loaded core. Indeed, the observed weight of the boron absorption in the BP is different in this case.

FIG. 11. Key factors in modelling and their impact on the reactivity for the 18 fuel columns core configuration (and full core)

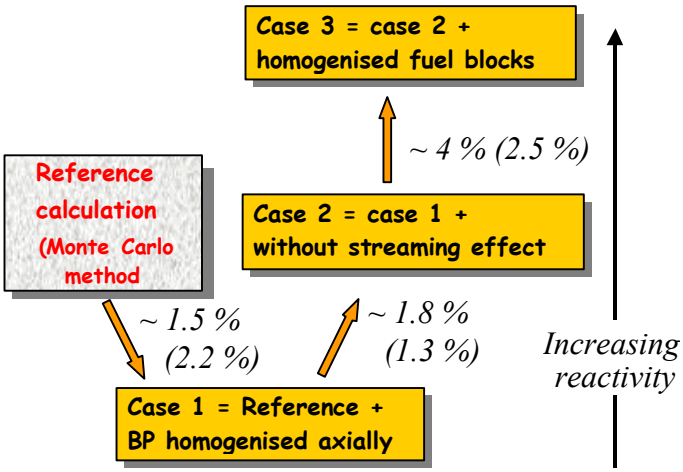

For the thin annular core, starting from a best estimate calculation and neglecting the fact that the burnable poison was axially a succession of boron and graphite pellets leads to a predicted reactivity 1.5 % lower than considering the actual heterogeneous composition of these burnable poisons (3D Monte Carlo estimation). On the opposite, a core calculation that does not take into account the streaming effect will result in an increase of the reactivity of about 1.8 %. At this stage, it is interesting to note that by making two strong physical hypotheses a result not far from the best estimate calculation can be obtained. Finally, a discrepancy on the order of 4 % can be achieved if an insufficient description of the fuel block is used to model the high level of radial heterogeneity (2D Monte Carlo estimation).

Therefore, the HTTR-FC2 benchmark has been a good opportunity to implement the new enhanced methods coming from this analysis and to evaluate the progress considering the new data.

HTTR-CR

Transport-diffusion calculations

The control rod insertion depths have also been evaluated to achieve criticality in the three configurations recommended by the benchmark problem HTTR-CR (thin and thick annular core and fully loaded core). The results corresponding to the *transport-diffusion* method are given in the following Table 3 with the calculational approach illustrated in Fig. 12.

TABLE 3 CRITICAL INSERTION DEPTHS OF THE CONTROL ROD

Configuration: Number of fuel columns	*Control rod critical positions from the bottom of the active core*
(thin annular core) 18	**251 cm**
(thick annular core) 24	**181 cm**
(fully loaded core) 30	**151 cm**

FIG. 12. Effective multiplication factor as a function of the control rod position

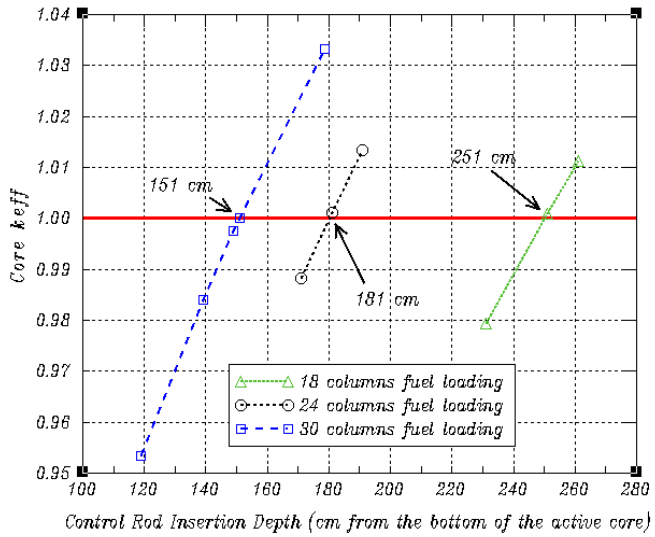

It should be noted that the core model used here does not allow taking into account the orientation of the control rods in the homogeneous block description, as it is also the case for the position of the burnable poison in the fuel element.

Transport-Monte Carlo Core Calculations

As far as the second method is concerned (*transport-Monte Carlo*) it is noteworthy that, as recommended by the benchmark problem, the structural materials of the control rod have not been taken into account. Conversely, a detailed axial description of the control rods has been done as depicted in Fig. 13.

FIG. 13. Axial Cross Section View of the Inserted Control Rods

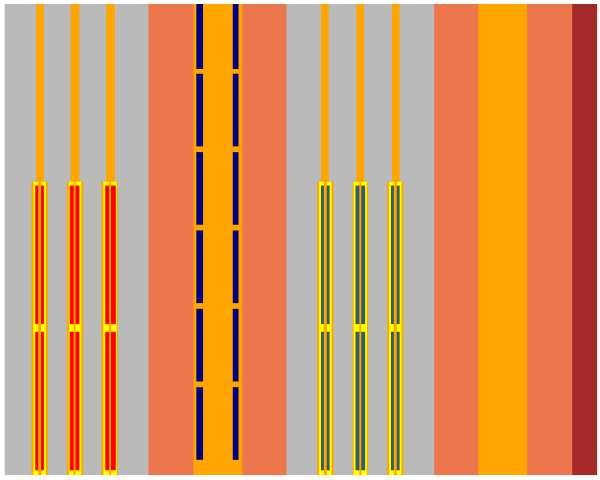

The calculations aimed to tentatively evaluate the critical insertion depth of the control rod in the fully loaded core configuration have been performed. Two control rod insertion depths have been considered. The first one -*178.7 cm*- is the experimental value and the second one -*170 cm*- comes from an estimation of the control rod efficiency obtained in the diffusion calculations. The results are given in the Table 4 below:

TABLE 4 REACTIVITY FOR TWO CONTROL ROD POSITIONS (FULL CORE)

Configuration: Number of fuel columns	*Control rod position from the bottom of the active core*	k_{eff}
(fully loaded core) 30	**178.7 cm**	**1.00850±0.0009**
(fully loaded core) 30	**170.0 cm**	**0.99840±0.0009**

From the results above, the critical rod position can be evaluated to **171 cm**. As a conclusion, one can note that, compared with the Monte Carlo, the control rod worth is overestimated with the diffusion method (without utilizing equivalence factor).

MODIFICATION TO MODEL AND ASSESSMENT OF IMPROVEMENTS

NEW FINITE ELEMENTS IN THE CORE DIFFUSION MODEL

New finite elements recently implemented in CRONOS-2 have been used. They allow taking into account the exact position of the burnable poison in the fuel blocks and the fuel element orientation in the core.

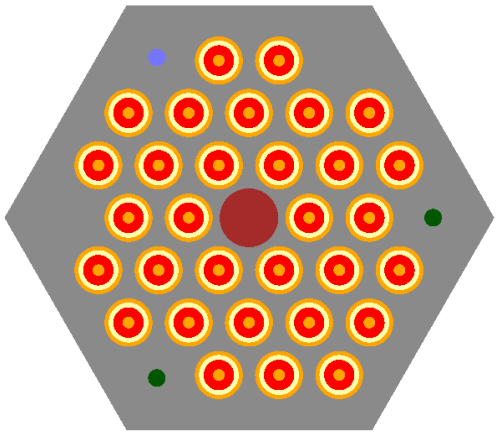

Fuel element geometry

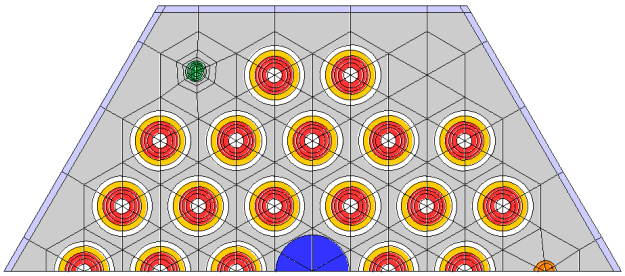

Fuel element description
in transport calculations (APOLLO2)

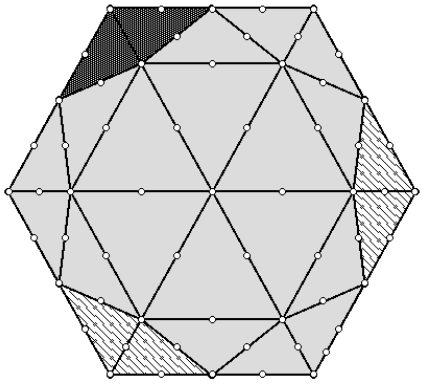

Fuel element description
in diffusion calculations (CRONOS2)

FIG. 14. Fuel element modelling in the improved Transport – Diffusion calculation scheme

Indeed, from the 2D transport calculations illustrated on the Fig. 2, the fuel element was initially homogenised in one hexagonal finite element. Then, with the help of the new available finite

elements, two different meshes were considered to describe the fuel elements with 24 radial meshes: 24 equilateral triangles (type I) or the cutting out depicted in Fig. 14 (type II). Only the last one has been kept in the final model because of the fact that it is the only one that allows homogenising the poison with its associated graphite without homogenising partially the fuel compacts. Therefore, the fuel element structure is described by using three different mediums and the flux is calculated for each point described in Fig. 14 (61 points for the hexagonal element).

When such a heterogeneous fuel block geometry is used in the diffusion calculations, the impact have been evaluated for the three core configurations with 18, 24 and 30 columns, on the basis of a 2D simplified core with no axial leakage and with an average uranium enrichment. The diffusion calculations are compared to the Monte Carlo one. The results obtained for the first configuration are presented in Fig. 15.

FIG. 15 2D calculation comparison for different energy group structure in the diffusion calculation - 18 columns core -

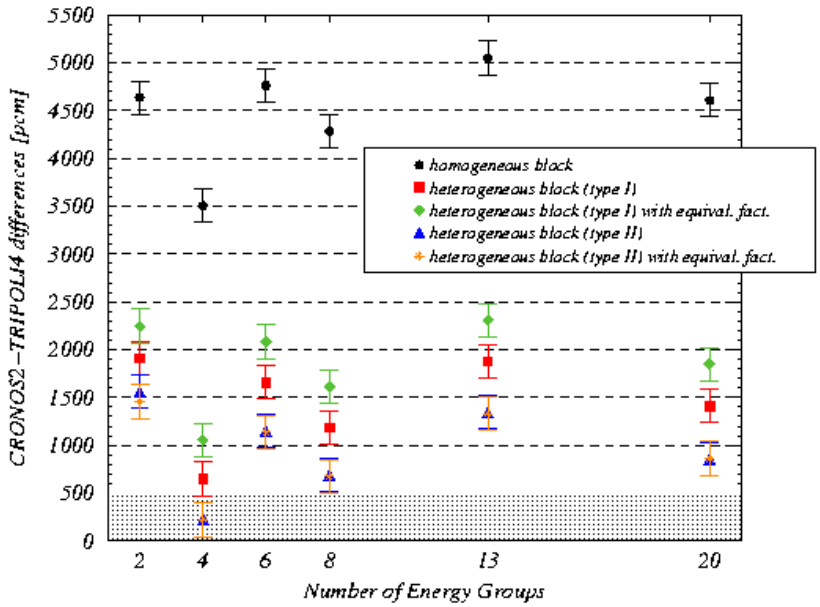

As previously mentioned, the most important impact is obtained for the 18 columns core loading. As far as the **full core** is concerned, the diffusion-Monte Carlo 2D-discrepancies become **quite acceptable** with the use of the new finite elements. Moreover, the use of equivalence factors has been implemented in order to respect the global absorption rate between the APOLLO-2 transport calculations (172 groups) and the CRONOS-2 diffusion calculations with few groups. This option has not been considered afterwards because of it small impact (Fig. 15) on the finite element of type II.

As a conclusion, a detailed description of the fuel block improves largely the results by giving a higher weight to the BP absorption in the fuel blocks. It allows getting quite acceptable values comparing to the reference TRIPOLI4 2D-calculation for the full core but a remaining discrepancy of about 1% can be observed for the annular core. This could be attributed to the cross section generation stage where the environment of the BP would not be representative of the one existing in the annular core configuration. Indeed, in this configuration the BP is surrounded by much more graphite (reflector) that thus increases the absorption flux-weighted cross-section. Besides, it would

appear that there is actually no specific trend concerning the energy structure to be retained in the CRONOS-2 calculations.

STREAMING MODELLING IN THE TRANSPORT CALCULATIONS

For improving the Transport – Diffusion calculation scheme, the streaming effect has been taken into account by using **anisotropic diffusion coefficients** in the core calculations. These diffusion coefficients have been evaluated in the fuel element transport calculation performed by APOLLO2. The Benoist method [9] available in APOLLO2 (called *TIBERE* model) is based on the B1 heterogeneous neutron leakage model. However, it might not be applicable in the large HTTR channels of the control rod graphite blocks (three large channels per block). Therefore, another analytical model (Benoist [10]) has also been tested on one control rod block alone and compared to the *TIBERE* model. With this formulation, the corrected diffusion coefficient is given by:

$$\frac{D_k}{\frac{1}{3}\lambda_m} = 1 + \frac{V_c}{V_t}\left(1 + \frac{c}{\lambda_m} Q_k\right) \qquad (1)$$

where:

- $Q_r = 1 - 1/\Delta \quad Q_Z = 2 - \frac{3\pi}{4} B_Z c \qquad k = r, z \qquad$ *(radial or axial)*
- c is the channel radius, λ_m is the mean free path of the moderator (graphite)
- $V_c = \pi c^2$ is the channel volume, V_t is the cell volume, B_Z is the axial buckling

and: $\Delta = \dfrac{\gamma}{\gamma + 1 - \dfrac{2b'}{1 - b'\dfrac{V_c}{V_t}}}$, $b' = \dfrac{\gamma + \frac{1}{2}}{\gamma + 1}$, $\gamma = \dfrac{c}{\lambda_m}$

In order to validate these models (*TIBERE* and analytical model), Monte-Carlo and diffusion calculations have been performed on the simplified geometry: the control rod block is surrounded by fuel elements and the axial structure of the geometry is the same as HTTR's core. The results are gathered in TABLE 5.

TABLE 5 STREAMING EFFECT CALCULATED ON THE SIMPLIFIED CORE

	TRIPOLI4	**CRONOS2**	
	$k_{effectif} \pm 3\sigma$	**2 gr.**	**8 gr.**
Homogeneous control block	1,27958 ± 0,00090	1,26320	1.27397
Heterogeneous control block			
TIBERE	1,27247 ± 0,00100	1,26040	1,27057
Analytical formulation		1,25657	1,26672
Streaming effect [pcm]			
TIBERE		222	267
Analytical formulation	560 ± 135	526	570

The streaming effect calculated by CRONOS2 is underestimated when the anisotropic diffusion coefficients are evaluated by the *TIBERE* model. The underestimation of the streaming effect is the consequence of a non-adequate calculation of the axial diffusion coefficient (underestimation of – 20 to – 25 % on D_z calculation). On the other hand, the use of an analytical model for the axial diffusion coefficient allows obtaining results in good agreement with the reference (Monte-Carlo method).

NEW RESULTS

NEW AVAILABLE DATA

The new data benchmark (HTTR-FC2) has been defined by JAERI [7]. It has been a good opportunity to implement the new enhanced methods coming from the previous analyses. Besides, the impact of these new data on the reactivity has been evaluated on the basis of the Monte Carlo calculations and of the improved core diffusion calculations. These effects are listed in Table 6.

TABLE 6 ANALYSIS OF THE BENCHMARK DATA IMPACT ON THE RESULTS

	Number of fuel columns	
	18	**30**
Residual air in the graphite porosity and re-evaluated impurities in the dummy fuel blocks	– 0.82 % (1)	– 0.3 % (1)
Worth of the CR insertion to the top of the reflector (R2 group)	– 0.22 % (1) – 0.32 % (2)	– 0.25 % (2)
Temporary neutron detector	non evaluated	non evaluated

(1) *Evaluated with the Transport – Monte-Carlo calculation scheme*
(2) *Evaluated with the Transport - Diffusion calculation scheme*

The overall effect can exceed 1 % according to the core configuration. One can note that the impact of the residual air in porosities and the impurities in graphite are much more higher in the thin annular core configuration. This could explain the decrease of the discrepancies between the experiment and the first calculation results, correlated to the number of dummy fuel blocks (graphite) discharged during the criticality approach.

DIFFUSION CALCULATION RESULTS

As far as the diffusion calculations are concerned, new developments carried out in APOLLO2 and CRONOS2 take into account:

- the exact position of the BP in the fuel block, by using new finite elements mesh in the core model
- the streaming effect, by generating anisotropic diffusion coefficients from both 2D-Pij calculations and analytical formulation.

The use of the HTTR-FC2 data associated with a complete description of the axial heterogeneity of the BP poison led to new core diffusion calculation results. This was done for several energy

structures in CRONOS2 without observing a main trend which would allow to select a reference as energy mesh.

The final results are partially gathered in Fig. 16 and 17. Figure 16 illustrates, with 8 energy groups, the impact of the different model assumptions on the reactivity as a function of the number of fuel columns loaded into the core. Figure 17 shows a streaming effect ranging from 2.25 % in the 18 columns core configuration to 1.8 % in the full core configuration. These results highlight also the importance of the used leakage model for evaluating the neutron streaming in the control rods graphite blocks. Indeed, the first model (*TIBERE* model) gave some values varying from 1.8 to 1.5 %.

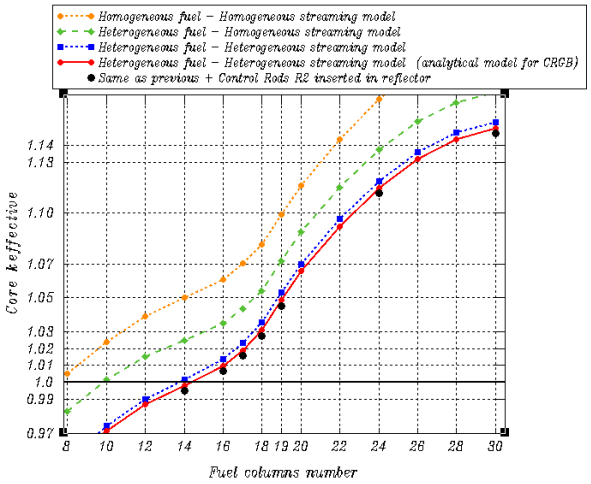

FIG. 16 k_{eff} values obtained with different core models

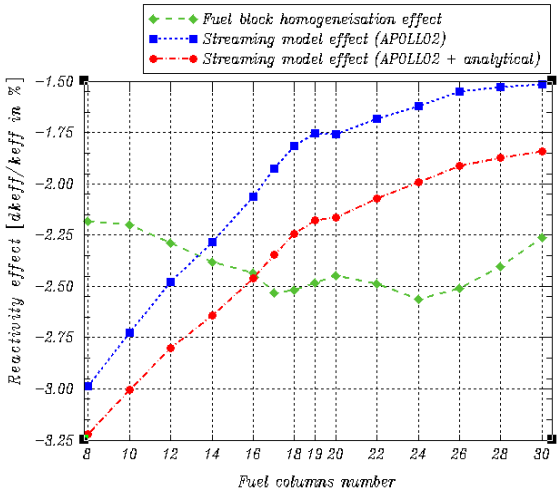

FIG. 17 Neutron streaming and fuel block homogenisation effect

It is noticeable that the number of fuel columns needed to achieve criticality increases by about 7 in comparison with the first results (Table 2) when considering the presence of the detectors and the CR inserted in the upper reflector. However, at first criticality, a discrepancy remains between the diffusion and the Monte-Carlo calculations (0.9 % < Δk/k < 1.7 %). This underscores the limits of a method based on a cross section homogenisation from a fundamental mode calculation (infinite medium) that is barely pertinent for the 18 columns core configuration. The actual environment (reflector blocks) should be considered and should take place instead of the white boundary condition in the 2D APOLLO2 transport calculations, before homogenising and collapsing locally the cross sections inside the fuel element.

FINAL RESULTS OF THE HTTR-FC2 PROBLEM

All the final results are gathered in Table 7. In the case of the Monte Carlo code TRIPOLI4, the discrepancy between the measurement and the calculation for the 18 fuel columns configuration is reduced to Δk/k ~ 0.8 %, when considering the revised data of the HTTR benchmark.

As far as diffusion calculations are concerned, the discrepancy is now reduced to Δk/k ~ 2.7 or 1.7 % (depending on the number of energy groups), when taking into account the improved models and the revised data. After all, it must be stressed that all the calculation results

obtained for the fully loaded core configuration fit the experiment, especially if one consider the experimental uncertainties.

TABLE 7 EXPERIMENTAL, MONTE-CARLO AND FINAL DIFFUSION RESULTS

	TRIPOLI4 [1] *3D Monte Carlo 172 gr & pointwise*	**CRONOS2** [1] **(Final model)** • 3D *Diffusion* • *4 groups - 8 groups*	**EXPERIMENT**
30 col.	1.13833 ± *0.00090*	1.1362 - 1.1451	1.1363 ± (> *3.6 %)*
24 col.	*	1.1000 - 1.1096	1.0834 ± (> *2 %)*
19 col.	1.02692 ± *0.00043*	1.0351 - 1.0432	1.0152 ± ?
18 col.	1.00855 ± *0.00090*	1.0178 - 1.0275	subcritical

[1] *detector impact included (Δk = 0.002) but not modelised*

EXCESS REACTIVITY HTTR-EX

All the excess reactivity are gathered below according to the previous values and the definition of the excess reactivity given in [2].

TABLE 8 EXCESS REACTIVITY FOR DIFFERENT CORE CONFIGURATIONS

Excess Reactivity [1]	**Number of loaded fuel columns**			
$(k_{eff} - 1)/k_{eff}$ [%]	**18**	**19**	**24**	**30**
Diffusion	1.7 < Δk/k < 2.7	3.4 < Δk/k < 4.1	9.1 < Δk/k < 9,9	12,0 < Δk/k < 12,7
Monte-Carlo	+ 0.85	+ 2.6	Non evaluated	+ 12,15

[1] *detector impact included (Δk = 0.002) but not modelised*

CONTROL ROD POSITION FOR CRITICALITY: HTTR-CR

The results presented in Table 9 correspond to the fully loaded core configuration. The control rod positions for obtaining criticality with all the inserted CR are: **178.7 cm** with the diffusion calculations and **177.9 cm** with Monte-Carlo code.

TABLE 9 k_{EFF} FOR DIFFERENT CR INSERTION DEPTHS. FULL CORE.

Control Rod Insertion Depth [cm]	**APOLLO2 – TRIPOLI4**	**APOLLO2 – CRONOS2**	**Exp.**
178,9	1,00117 ± 0,00024	1,00020	critical
177,6	0,99972 ± 0,00038	0,99840	*

It is noteworthy that the CR insertion depth is well evaluated with the diffusion core calculation despite of the discrepancies with the Monte Carlo results observed in this configuration without the inserted CR. This remark underscores the fact that the CR worth is overestimated with the diffusion method especially in this case where no equivalence factors have been used in order to respect

either the flux or the absorption rates between the multi-group transport calculations and the broad group diffusion core calculations.

SCRAM REACTIVITY: HTTR-SC

In this section, the CR worth has been evaluated (Table 10) in the fully loaded core configuration and according to:

$$\rho = \frac{k_{crit.} - k_{Control\ Rods\ IN}}{k_{crit.} \times k_{Control\ Rods\ IN}}$$

As far as the CR insertion in the reflector is concerned, an unexplained result has been observed with the Monte Carlo calculation, whilst a good agreement can be observed for the overall CR worth inserted in the core. Once again, these results highlight the overestimation of the absorbant in the diffusion calculation when one compares the CRONOS2 results to those of TRIPOLI4.

TABLE 10 CONTROL ROD WORTH

	TRIPOLI4 (Monte Carlo)	CRONOS2 (diffusion)	Exp.
CR inserted in the reflector			
$\mathbf{k_{critique}}$	1,00117 ± 0,00024	1,00020	*
$\mathbf{k_{RCR}}$	0,92215 ± 0,00040	0,90245	*
$\mathbf{\rho_{RCR}}$ **[%]**	**8,56**	**10,83**	**12,0 ± 1,2**
All the CR inserted in the core			
$\mathbf{k_{critique}}$	1,00117 ± 0,00024	1,00020	
$\mathbf{k_{RCR}}$	0,68396 ± 0,00030	0,63982	
$\mathbf{\rho_{RCR}}$ **[%]**	**46,32**	**56,31**	**46,0 ± 4,6**

ISOTHERMAL TEMPERATURE COEFFICIENT IN THE CORE : HTTR-TC

The temperature coefficients have been evaluated from the following expression:

$$\rho_{12} = \frac{k_{T_1} - k_{T_2}}{k_{T_1} \times k_{T_2}} \cdot \frac{1}{(T_1 - T_2)}$$

They have been estimated only from k_{eff} of the core diffusion calculations performed at different temperature (Table 11).

TABLE 11 K_{EFF} AS FUNCTION OF THE TEMPERATURE

Temperature [K]	APOLLO2 – CRONOS2
300	1,00395
340	0,99724
380	0,99088
420	0,98455
460	0,97823
480	0,97525

According to the results gathered in Table 12, the temperature coefficients range from - 15 to - 16 pcm/°K between 300 to 420 K.

TABLE 12 ISOTHERMAL TEMPERATURE COEFFICIENTS

Temperature coefficients [pcm/°K]	APOLLO2 – CRONOS2
ρ_{320}	– 16,75
ρ_{360}	– 16,09
ρ_{400}	– 16,22
ρ_{440}	– 16,40
ρ_{470}	– 15,62

CONCLUDING REMARKS

The HTTR's core physics benchmarks have been treated with two different calculation scheme: a transport-diffusion method and a transport-Monte Carlo one. These benchmarks constitute the first opportunity in reactor physics to model and benchmark the codes and methods in thin **annular core geometry**. This important point led to the limitations of the classical two-steps core modeling based on a transport-diffusion chained calculations in order to take accurately into account the **core/reflector interface**. Moreover, one of the other characteristics of the HTTR core in its annular configuration was the presence of a large number of uncommon **big channels** offering the possibility for the neutrons to leak from the active zone (*streaming effect*). In addition to that, the **important axial and radial heterogeneities** in the core (burnable poison, many different enrichments) make the HTTR a real challenge in reactor physics.

Quite acceptable results are obtained in the **fully loaded core configuration**. Besides, some **discrepancies** between the calculations and the experiment appear for intermediate core configuration (**thin annular core**) close to criticality. Parts of these discrepancies were reduced to **$\Delta k/k \sim 0.85$ %** with the Monte-Carlo calculations taking into account the new benchmark data (air in porosity and impurities in graphite). As far as the deterministic approach is concerned, the discrepancies were analysed and tackled by different treatments. However, a difference of at least **1 %** remains between the diffusion and the Monte Carlo calculations in the **annular core** configuration when considering revised data.

REFERENCES

[1] N. NOJIRI, M. NAKANO, N. FUJIMOTO, K. YAMASHITA, M. TATEUCHI, S.FUJISAKI, S. YOSHIMUTA, K. SAWA, M. SATO, M. ISHIHARA, T. IYOKU, H. SAWAHATA, *« Benchmark problem's data for the HTTR's start-up core physics experiments »*, January, 1998

[2] K. YAMASHITA, N. FUJIMOTO, M. NAKANO, U. OHLIG, *« IAEA Benchmark Calculation results of the HTTR's start-up core physics tests »*, JAERI report, memo 11-030. March, 1999

[3] R. SANCHEZ, A. HEBERT, Z. STANKOVSKI, M. COSTE, S. LOUBIERE, C VAN DER GUCHT and I. ZMIJAREVIC, *« APOLLO2 Twelve Years Later »*, Mathematics and Computation, Reactor Physics and Environmental Analysis in Nuclear Applications, Madrid, September, 1999

[4] J.J. LAUTARD, S. LOUBIERE, C. MAGNAUD *« CRONOS, A Modular Computational System for Neutronic Core Calculations »*, IAEA Specialists Meeting, France, September, 1990

[5] J.P. BOTH, Y. PENELIAU, *« The Monte Carlo code TRIPOLI4 and its first benchmark interpretations »*, International Conference PHYSOR 96, Mito, Ibaraki, Japan, September, 1996

[6] 2nd Research Coordinated Meeting of IAEA CRP-5, *« Evaluation of High Temperature Gas-cooled Reactors »,* Beijing, China, October 18-22, 1999

[7] N. FUJIMOTO, *« Data for re-calculation of HTTR-FC »,* November, 2000

[8] F. MOREAU, R. SANCHEZ, S. SANTANDREA, *« Contribution to the NEA C5G7 MOX benchmark »*, International Conference PHYSOR 2002, Seoul, South Korea, October, 2002

[9] I. PETROVIC, P. BENOIST, *« B_N Theory: Advances and New Models for Neutron Leakage Calculation »*, Advances in Nuclear Science and Technology, Plenum Publishing Corporation, New York, vol. 24, 1996

[10] P. BENOIST, J. MONDOT, I. PETROVIC, *« Calculational and experimental investigations of void effect. A new model for leakage treatment of heterogeneous assemblies »*, Nuclear Science and Engineering, 118, 197, 1994.

[11] N. NOJIRI, N. FUJIMOTO, K. YAMASHITA, *« HTTR's Benchmark Calculation of Start-up Core Physics Tests»*, January 1998

[12] N. FUJIMOTO, K. YAMASHITA, M. NAKANO, M. TATEUCHI, S.FUJISAKI, *« Experimental Results of HTTR's Start-up Core Physics Tests »*, 2000.

[13] N. FUJIMOTO et al. *« Control Rod Position and Temperature Coefficients in HTTR Power-Rise Test »*, JAERI Tech 2000-091 (2000).

ANNEXE

Several energy structure have been tested in course of this study for the core diffusion calculations : the 2, 4, 8 and 20 group meshes, currently applied in the PWR studies and the 6 and 13 groups which have already been used in the GT-MHR related analyses.

13 gr	6 gr	Limite inférieure en énergie [Mev]
1	1	$1,8315,10^{-1}$
2	2	$1,0104,10^{-3}$
3		$1,6745,10^{-5}$
4	3	$4,1293,10^{-6}$
5		$2,13,10^{-6}$
6	4	$1,305,10^{-6}$
7		$7,90,10^{-7}$
8		$6,2501,10^{-7}$
9	5	$3,91,10^{-7}$
10		$3,145,10^{-7}$
11		$1,15,10^{-7}$
12	6	$5,9,10^{-10}$
13		$1,1,10^{-10}$

The 6 and 13 group structures

8 gr	4 gr	2 gr	Limite inférieure en énergie [Mev]
1	1	1	$9,0718,10^{-1}$
2	2		$2,7324,10^{-3}$
3			$5,0045,10^{-3}$
4	3		$2,7679,10^{-6}$
5			$1,67,10^{-6}$
6			$6,2501,10^{-7}$
7	4	2	$1,6,10^{-7}$
8			$1,1,10^{-10}$

The 2, 4 and 8 group structures

20 gr	Limite inférieure en énergie [Mev]	20 gr	Limite inférieure en énergie [Mev]
1	4,493	11	$5,560.10^{-5}$
2	2,231	12	$4,000.10^{-6}$
3	1,353	13	$6,250.10^{-7}$
4	$4,979.10^{-1}$	14	$3,500.10^{-7}$
5	$1,832.10^{-1}$	15	$2,200.10^{-7}$
6	$6,738.10^{-2}$	16	$1,340.10^{-7}$
7	$2,479.10^{-2}$	17	$7,700.10^{-8}$
8	$9,119.10^{-3}$	18	$3,000.10^{-8}$
9	$2,035.10^{-3}$	19	$1,000.10^{-8}$
10	$4,540.10^{-4}$	20	$1,1.10^{-10}$

The 20 group structure